On the Cylinder Collapse Problem, Mixing, and the Merger of Isolated Eddies

WILLIAM K. DEWAR

Department of Oceanography, Florida State University, Tallahassee, Florida

PETER D. KILLWORTH

Institute of Oceanographic Sciences, Deacon Laboratory, Wormley, Godalming, Surrey and Hooke Institute for Atmospheric Research, Dept. of Atmospheric, Oceanic and Planetary Physics, Clarendon Laboratory, Oxford, England

(Manuscript received 22 May 1989, in final form 21 December 1989)

ABSTRACT

The Rossby adjustment of an initially circular column of water, the so-called collapse of a cylinder, continues to be a widely used method for forming lenslike eddies in the laboratory. Here, we consider the structure of an eddy so formed as well as some ramifications of that formation. We demonstrate that the calculation of the eddy structure can be reduced to the extraction of the roots of two nonlinear, coupled algebraic equations. Analytical solutions in the limit of the collapse of a needle are given and roots are obtained numerically otherwise. It is concluded that in the collapse of a cylinder initially spanning the entire column of water, the eddy always maintains contact with both surfaces. (This is not the case in the seemingly equivalent two-dimensional case with no variation in one Cartesian direction.) In the event the initial cold column is separated only slightly from the surface, the above solution acts as the lowest order solution in a regular perturbation sequence.

Next, these "collapse eddy" solutions, which possess motions in both layers and finite energies, are used to examine lens merger. Two collapse eddies of equal volume jointly possess less energy than one collapse eddy of twice the volume. However, we argue that two collapse eddies of equal volume can have more energy than the circularly symmetric end-state eddy formed from them if the two initial eddies "mix." We also offer evidence that the energy budgets may be balanced exactly if the end-state eddy is slightly asymmetric. Comparisons with some previous laboratory experiments are made.

1. Introduction

Eddies are a ubiquitous feature of the ocean and continue to be the objects of much scrutiny theoretically, observationally, and in the laboratory. Many of the eddies of interest are decidedly discrete in nature resembling finite volumes of anomalous water imbedded in a host background. Examples are warm core rings and submesoscale coherent vortices. Much has been recently learned about them in the field due to a few intensive observational programs (McWilliams et al. 1983; Joyce 1985). In contrast, several basic dynamical questions remain unanswered about lens structure and interaction, both in theory and in the laboratory setting. The purpose of this paper is to contribute to the latter topics, namely; the structure of "thick" lenses is considered and the conditions under which two such eddies might coalesce are examined.

Background. Of the many possible types of lens interactions one that has drawn significant recent attention is that of lens–lens merger. The clearest observational evidence of such an interaction was obtained by Cresswell (1982) in the East Australia current system. He interpreted two hydrographic surveys as indicative of the coalescence of two warm eddies possessing slightly different densities. Given the relatively restricted regions in which such eddies are found (i.e., usually in the vicinity of major current systems), one expects that vortex interactions are numerous, and determining the conditions under which merger will occur is of obvious interest.

In what has become the classic work in this area Gill and Griffiths (1982) pointed out that simple lens merger in reduced gravity models was not energetically permissible. They demonstrated that two zero potential vorticity eddies of a given volume possessed less energy (by roughly 40%) than one zero potential vorticity eddy of twice the volume. Viewing the latter as an end state of the merger process, they posed what has since become the fundamental question of lens–lens merger; namely, what are the conditions under which two lenses coalesce?

Subsequent numerical and laboratory studies of vortex–vortex interaction have demonstrated that two like-signed vortices will merge under a wide variety of conditions and dynamics (Overman and Zabusky 1982; Mied and Lindermann 1984; Melander et al. 1985; Griffiths and Hopfinger 1986, 1987; Nof and

Corresponding author address: Department of Oceanography, Florida State University, Tallahassee, Florida 32306.

Simon 1987). In none of these examples were external energy sources supplied, so all of them had to overcome the Gill and Griffiths constraint internally. In Euler equation experiments, vortex merger was accompanied by filament formation, and these were shown to be crucial in restoring global energy and mass balances. Griffiths and Hopfinger argue for geostrophic eddies that the kinetic energy in the eddy exterior could be used to balance energetics and they also discussed the role of spiral arms in merger. (Note f-plane solutions for baroclinic vortices like those discussed by Griffiths and Hopfinger are unbounded in space and have infinite kinetic energy.) Nof (1988) argues for the case of lens merger that the coalescence mechanism involves mutual intrusions by the eddies and that shock waves formed on the lead edge of the intrusions alter eddy potential vorticity. He points to the coalescence observed in Nof and Simon (1987) and the attendant restructuring of the resultant eddy as an example of this process. More recently Cushman-Roisin (1989) has examined the role of spiral filaments in lens coalescence and shown how energy, angular momentum, and mass budgets can be satisfied by their inclusion. He further suggests that filaments are relatively fine and are thus easily masked in the laboratory by diffusion and friction.

A common theme of the Nof and Cushman-Roisin arguments is that they are essentially imbedded in the reduced gravity equations. This discards the possible impact of external flow in any of the balances, thus eliminating the kinetic energy conversion mechanism proposed by Griffiths and Hopfinger. Of course the latter were not working with isolated lenses, and the presence of an infinite kinetic energy in quasi-geostrophic eddies complicates the examination of energy budgets.

In this paper we examine the structure of lenses formed by the collapse of cylinders (lenses so formed are here named "collapse" eddies). As demonstrated by Nof and Simon (1987) this is a robust way of generating finite volume lenses in the laboratory. We calculate the motion in both layers, and the solutions are offered to aid in the analysis of future laboratory experiments on lenses. The energetics of these solutions are then analyzed with a view to determine if the energetic prohibitions against lens merger are removed when an active second layer is taken into account. In contrast to the Griffiths and Hopfinger analysis, these collapse eddies possess finite velocity distributions and, hence, the role of kinetic energy conversion can be different than the quasi-geostrophic case.

Accordingly, we find that collapse eddies are rather remarkable in structure. Specifically, if the initial cylinder extends through the full layer of water, the collapse eddy must have a point of contact with both the surface and the bottom. (On the other hand, this does not hold for the apparently related collapse problem in a strip.) The velocity in the exterior fluid is significant, but entirely contained within the vicinity of the collapse eddy. The total energy of this configuration is dominated by potential energy. The structure of the collapse eddy formed from cylinders, which reach "almost" through the layer of water, is shown to represent a regular perturbation problem about the former solution.

The total energy in two collapse eddies of a given volume V_0 is less than the total energy of a single collapse eddy of volume $2V_0$, thus demonstrating that a collapse eddy is not an allowable end state of merger. On the other hand, if the collapse eddies are assumed to "mix" in a simple way, a parameter range is found for which the end state eddy with volume $2V_0$ has less total energy than the initial state. The mixing parameterization employed is simply a volume averaging of potential vorticity. We argue that the potential vorticity distributions, so formed, are necessary to obtain a realizable time-independent eddy.

A major effect on the energy budgets is the release of potential energy caused by mixing. Commensurate with this is a significant structural change of the eddy. The results of the analysis are compared with the experiments of Nof and Simon (1987), and evidences of mixing and the required thermocline change are pointed out.

Thus, we suggest that vortex merger can be affected by external flows, but in a manner different from that proposed by Griffiths and Hopfinger (1986). The process of merger can disrupt the integrity of the external flow and this, in turn, can provide a mechanism for release of potential energy, thus allowing merger to be possible.

The collapse eddy solution is examined in the next section and the solutions for the so-called mixed eddy states are presented in section 3. An examination of merger, comparison with laboratory experiments and a discussion of the results close the paper.

2. The collapse of a cylinder

The problem simply stated is to compute the steady cyclostrophically balanced flow that would evolve from the collapse of an initially cylindrical column of cold water. A Boussinesq fluid is assumed and frictional effects are neglected. [In a related paper Smeed (1987) has calculated an approximate structural solution for a two-layer eddy formed by the collapse of an initially unbalanced mass of warm water. The lower layer in his model is set into motion by the adjustment and interacts frictionally with the bottom. Smeed used this model to analyze laboratory experiments on the effects of Ekman transport in benthic frontogensis.] It is also assumed that the height of the cold column matches that of the surrounding warm water and that the fluid is everywhere initially motionless (see Fig. 1a). Further, the fluid is contained between two rigid surfaces, and the system is rotating at a fixed rate proportional to f.

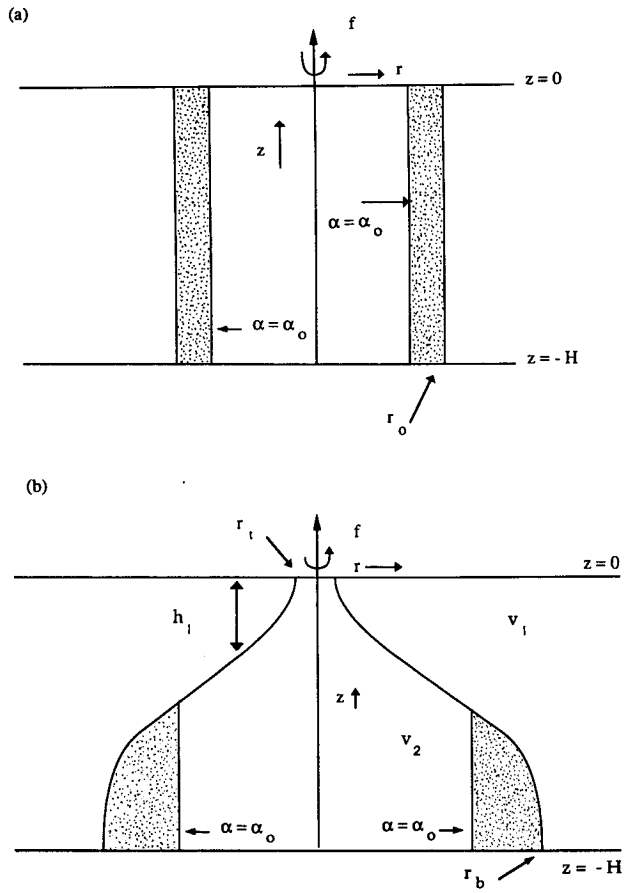

FIG. 1. Collapse schematic. The state prior to collapse is shown in (a). The initial radius of cold water is denoted by r_0 and the total fluid depth is H. The collapsed state is shown in (b). The thermocline point of contact with the surface is denoted r_t and that with the bottom is denoted r_b. The shaded areas indicate the conservation of volume enclosed by angular momentum surfaces.

The radius of the initial column is denoted r_0. This initial state is chosen in view of the eddy formation techniques employed in Nof and Simon (1987).

The final adjusted state of the system is schematically depicted in Fig. 1b. The variable h_i denotes thickness, v_i azimuthal velocity, and the subscript i denotes the ith layer ($i = 1$ denotes upper layer, $i = 2$ denotes lower). The possibility of outcrop locations on both boundaries is included in Fig. 1b; the location of the inner outcrop on the upper surface is denoted r_t and the outcrop on the bottom is located at r_b.

The equations governing the final, steady upper and lower layer fields are the cyclostrophic equations:

$$\frac{v_1^2}{r} + fv_1 = P_{2r} + g'h_{1r} \tag{1a}$$

$$\frac{v_2^2}{r} + fv_2 = P_{2r} \tag{1b}$$

which upon subtraction yield essentially the thermal wind equation:

$$\frac{v_1^2 - v_2^2}{r} + f(v_1 - v_2) = g'h_{1r}. \tag{2}$$

Layer thicknesses are connected by

$$h_1 + h_2 = H. \tag{3}$$

It should be noted that (1) depends only on the assumption that the final steady state is radially symmetric, in which case radial and vertical velocities vanish. If it is further assumed that the adjustment is symmetric, angular momentum $[\alpha_i = (rv_i + fr^2/2)]$ is conserved by fluid parcels throughout the adjustment process:

$$\frac{d}{dt}\left(rv_1 + \frac{fr^2}{2}\right) = \frac{d}{dt}\left(rv_2 + \frac{fr^2}{2}\right) = 0. \tag{4}$$

It should also be noted that (4) can be obtained by manipulation of the azimuthal momentum equation, and is thus true even in the presence of nonhydrostatic phenomena. Indeed, it is for this reason that we choose to work with angular momentum as the vigorous adjustment process is likely to be nonhydrostatic, at least initially. Denoting $r_{1,i}$ as the initial location of a warm parcel, and $r_{2,i}$ as the initial location of a cold parcel, it is possible using (4) to relate final velocities and final positions of parcels, viz:

$$rv_1 + \frac{fr^2}{2} = \frac{fr_{1,i}^2}{2} \tag{5a}$$

$$rv_2 + \frac{fr^2}{2} = \frac{fr_{2,i}^2}{2}. \tag{5b}$$

It is convenient to introduce the new variables:

$$p_1 = \frac{r_{1,i}^2}{2}, \quad p_2 = \frac{r_{2,i}^2}{2} \quad \text{and} \quad q = \frac{r^2}{2} \tag{6}$$

which leads to

$$v_1 = f\frac{(p_1 - q)}{\sqrt{2q}} \tag{7a}$$

$$v_2 = f\frac{(p_2 - q)}{\sqrt{2q}}. \tag{7b}$$

In terms of these variables, (2) becomes

$$\frac{f^2(p_1 - q)^2 - f^2(p_2 - q)^2}{4q^2} + \frac{f^2}{2q}(p_1 - p_2) = g'h_{1q}. \tag{8}$$

The problem now reduces to calculating the initial locations, p_i, of fluid parcels which in the final state are at location q.

A second conserved quantity (along with α) is material volume, and this is exploited by noting that sheets of constant α constitute material surfaces. Therefore, the volume of fluid inside a constant α surface can be evaluated from the initial conditions (see Fig. 1).

This constraint is expressed as

$$H\int_{p_0}^{p_1} dp_1 = \int_{q_t}^{q} h_1\, dq \tag{9a}$$

$$H\int_{p_2}^{p_0} dp_2 = \int_{q}^{q_b} h_2\, dq \tag{9b}$$

for the upper and lower layer, respectively. The quantity p_0 denotes $r_0^2/2$, $q_t = r_t^2/2$, and $q_b = r_b^2/2$ in the above. Differentiating (9) by q yields

$$Hp_{2q} = h_2 \tag{10a}$$

$$Hp_{1q} = h_1. \tag{10b}$$

Note from (10b) that $p_1 = q$ for $q > q_b$. This implies by (7a) that $v_1 = 0$ for $q > q_b$, or that all motion is contained within the area of the lens.

Summing (10), applying (3), and after a simple calculation the result

$$p_1 + p_2 = q + p_0 \tag{11}$$

is obtained. The above constant of integration has been determined by the boundary conditions $p_1 = q_b$, $p_2 = p_0$ when $q = q_b$ (see Fig. 1). Equation (8) can now be converted into one equation in p_1 by substituting with (11) and (10b). If p_1, p_2, and q are now nondimensionalized by $g'H/f^2$, i.e., the square of the deformation radius based on the total fluid depth, the nondimensional equation:

$$p_{1qq} - \left(\frac{1}{2} + \frac{p_0}{2q}\right)\frac{p_1}{q} = -\left(\frac{1}{2} + \frac{p_0}{2q}\right)^2 \tag{12}$$

is obtained. Its solution is most conveniently written by converting back to the radial coordinate r:

$$p_1 = r^2/4 + r_0^2/4 + ArI_a(r) + BrK_a(r), \tag{13}$$

where I, K are modified Bessel functions and

$$a = (1 + r_0^2)^{1/2}.$$

The constants A, B are fixed by the boundary conditions

$$p_1 = r_0^2/2, \quad r = r_t \tag{14a}$$

$$p_{1r} = 0, \quad r = r_t \tag{14b}$$

$$p_1 = r_b^2/2, \quad r = r_b \tag{15a}$$

$$p_{1r} = r_b, \quad r = r_b \tag{15b}$$

for as yet unknown values of r_t, r_b. Equations (14a, b) represent angular momentum conservation and (15a, b) represent outcrop conditions [see (10)]. Substitution of (13) into (14) gives, using properties of modified Bessel functions,

$$A = (r_0^2 - r_t^2)K_{(a-1)}(r_t)/4 + [(a-1)(r_0^2 - r_t^2)/(4r_t) - r_t/2]K_a(r_t) \tag{16a}$$

$$B = [(r_0^2 - r_t^2)/(4r_t) - AI_a(r_t)]/K_a(r_t). \tag{16b}$$

These values for A, B (in terms of the unknown r_t) can be substituted into (15) to give two equations in r_t and r_b:

$$AI_a(r_b) + BK_a(r_b) = (r_b^2 - r_0^2)/(4r_b) \tag{17}$$

$$AI_{(a-1)}(r_b) - BK_{(a-1)}(r_b) = 1/2 + (a-1)(r_b^2 - r_0^2)/(4r_b^2) \tag{18}$$

which, although nonlinear, are considerably simpler than the associated differential equations.

The analysis so far is exact, and the solutions of (17) and (18) can easily be obtained numerically. However, before presenting these results we investigate the asymptotic limit of $r_0 \ll 1$. Note from Fig. 1 that $r_t < r_0$. We assume explicitly that for small r_0, $r_t \sim r_0^2$ and will check later for consistency. Thus, we write $r_t = \gamma r_0^2$ for some unknown γ of order unity. The order a of the modified Bessel functions is then approximately $1 + r_0^2/2$. A, B are given to leading order from (16) by

$$A = -1/2 + 1/(8\gamma^2) \tag{19}$$

$$B = r_0^2/4. \tag{20}$$

Provided that r_b is larger than r_0, substitution into (18) gives

$$Ar_b = r_b/2 \tag{21}$$

to leading order, so that $A = 1/2$ and

$$\gamma = 1/(2\sqrt{2}). \tag{22}$$

Thus, $r_t = r_0^2/(2\sqrt{2})$, demonstrating that the initial assumption $r_t = O(r_0^2)$ is indeed consistent. Further,

$$p_1 \sim r^2/4 + r_0^2/4 + (r/2)I_a(r) + r_0^2K_a(r)/4 \tag{23}$$

to leading order. Given the above results, the swirl flow at r_t can be calculated. Angular momentum conservation requires

$$r_t v_t + r_t^2/2 = r_0^2/2 \tag{24}$$

so that $v_t = \sqrt{2}$, or dimensionally that $v_{t\text{dim}} = \sqrt{2}fR_d$.

The important point here is that the collapse eddy does not subduct, [cf. (22)] no matter how small r_0 is. This is in agreement with angular momentum conservation that would otherwise require infinite velocity in the warm fluid at $r = 0$. Note, however, that qualitatively different behavior emerges if the cylindrical geometry is replaced by cartesian geometry and the usual assumption about the independence of the solution on one of the coordinates is made (see the Appendix). In

that case a sufficiently narrow eddy does subduct. The difference in the behaviors can be traced to the difference in the geometries, and is most obvious in the definitions of angular momentum ($\alpha = rv + fr^2/2$ in the cylindrical system, and $\alpha = v + fx$ in the cartesian system).

Straightforward root-finding procedures work well on extracting the solutions of (17) and (18) for a given p_0. Here, we have used the subroutine hybrid1 from the software package MINPACK. Examples of the thermocline structure for several values of p_0 are shown in Fig. 2. Note that the collapse eddy thermocline resembles an inverted champagne glass. We also mention that the numerically calculated values for r_t and v_t support the asymptotic results in (22) and (24).

Capped eddy collapse

The structure of the collapse eddies is rather remarkable in that they maintain a point of surface contact. At this stage it might appear that this result is singular and dependent critically upon the initial cold water column filling the entire layer. Here, it is argued that the collapse eddy structure consistent with a column which only partially fills the layer passes smoothly to the solution in the previous section. Thus, the collapse eddy structure problem does not appear to be singular.

Consider the initial structure in Fig. 3a, which upon relaxation presumably assumes a structure like that in Fig. 3b. The parameter δ denotes the nondimensional thickness of the initial warm "cap" and p_0 denotes the initial cylindrical radius. Equations (2) and (3) still apply everywhere in the final state, but it is necessary to divide the warm fluid into two regions characterized by the nondimensional potential vorticity equations:

$$\frac{1}{r}\frac{\partial}{\partial r} rv_1 + 1 = \delta^{-1}h_1 \quad 0 < r < r_t \tag{25a}$$

$$\frac{1}{r\partial r} rv_1 + 1 = h_1 \quad r_t < r < \infty. \tag{25b}$$

The quantities r_t and δ are related by

$$\int_0^{r_t} h_1 r dr = p_0\delta, \tag{26}$$

and the location where h_2 vanishes is denoted as r_b. Boundary conditions of v_1 are that it vanish at $r = 0$, be continuous at r_t, and vanish at r_b. Upper layer thickness h_1 is also required to be continuous at r_t. Finally, the set of equations is closed by including lower layer potential vorticity,

$$\frac{1}{r}\frac{\partial}{\partial r} rv_2 + 1 = h_2(1 - \delta)^{-1}. \tag{27}$$

No method for solving the structure equation analytically in region I has been found; however, the above set composes a two-point boundary value problem and is simple to solve numerically. A two-parameter family of solutions can be generated by varying p_0 and δ.

A comparison of thermocline structures for $p_0 = 0.2$ and several nonzero values for δ are shown in Fig. 4. Also shown is a plot of h_1 calculated using the analytical

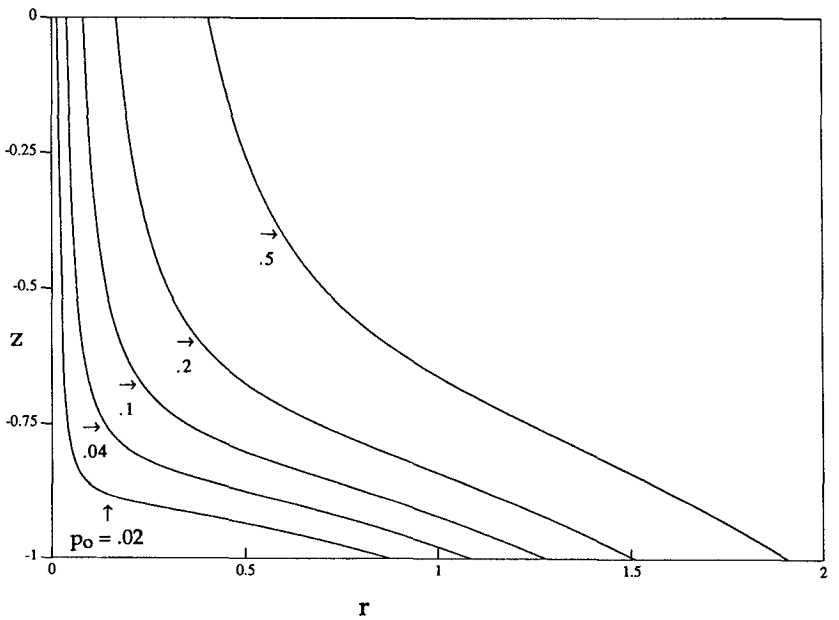

FIG. 2. Collapse eddy structure. Thermocline structure versus radial position is plotted for several values of p_0. Note the inverted champagne glass structure obtained for small p_0.

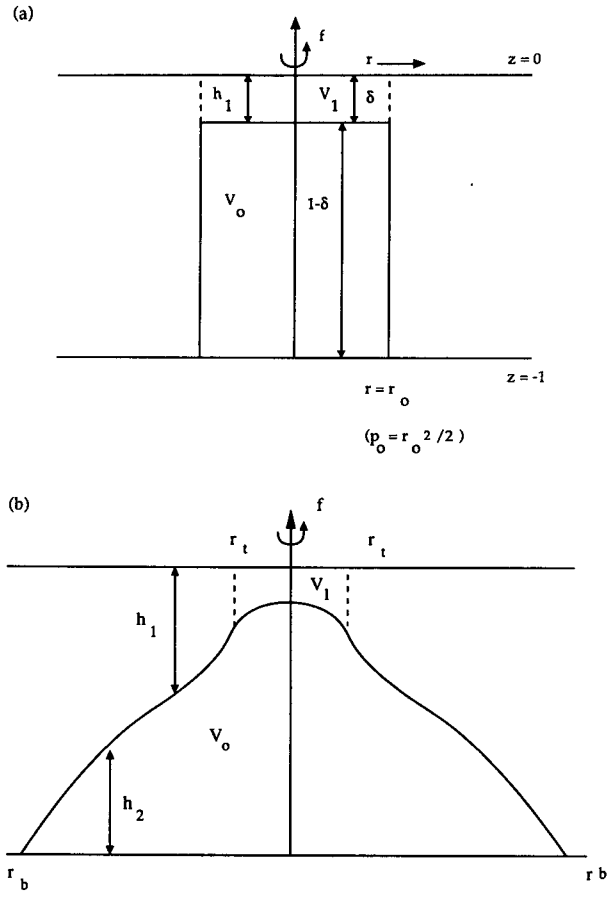

FIG. 3. Capped eddy collapse. The initial state is shown in (a) and the final state in (b). The quantity δ denotes the nondimensional initial thickness of the cap and p_0 the initial radius of cold water.

$\delta = 0$ solution. Small δ values lead to h_1 patterns which closely resemble the $\delta = 0$ solution, e.g., the tendency for the eddies to develop stems extending toward the surface.

It is also of interest to examine the energy of the collapse eddies as a function of δ. The total kinetic plus available potential energy of a collapse eddy in this problem is given by

$$E(p_0, \delta) = \int_0^{r_b} h_1 \frac{v_1^2}{2} rdr + \int_0^{r_b} h_2 \frac{v_2^2}{2} rdr + \int_0^{r_b} \frac{h_2^2}{2} rdr. \quad (28)$$

The quantity E depends on initial cylinder radius (effectively p_0) and cap thickness, δ, and has been calculated numerically for several collapse eddies. Typical results are shown in Fig. 5 for the choice $p_0 = 0.2$. The quantity δ varies between 0.2 and 0 with the point being that the total available energy in a collapse eddy is a smooth function of δ. This quantitatively supports the notion that the collapse problem is not singular.

As is usually the case in Rossby adjustment problems the total available energy of the initial unbalanced state is greater than the energy in the steady final state, i.e.,

$$E_{\text{initial}} = \frac{(1-\delta)^2}{2} p_0 > E(p_0, \delta).$$

This is unacceptable from a formal point of view as the inviscid rigid lid system, in which this problem is imbedded, conserves energy. The complete solution of this initial value problem must also involve a time dependent part (presumably inertial oscillations) which

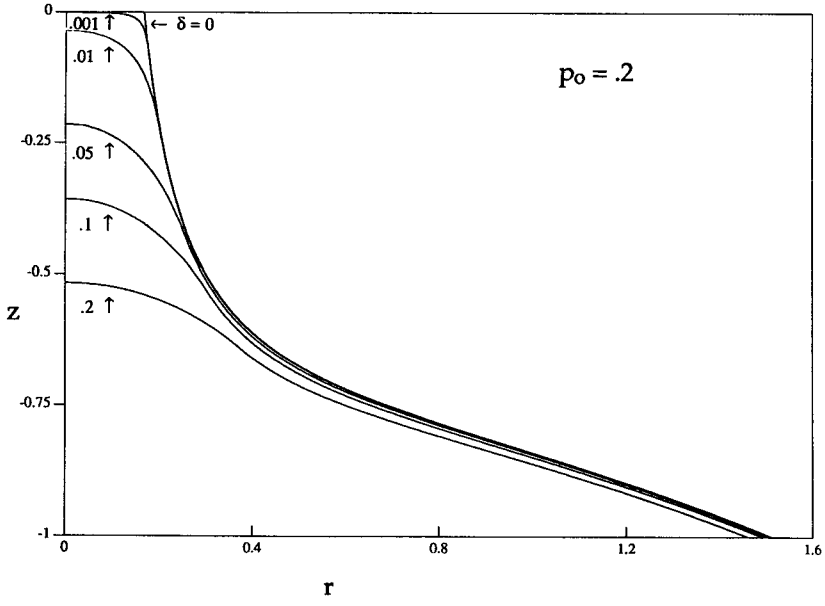

FIG. 4. Thermocline structure for $p_0 = 0.2$ and several values of δ. Note that the structure smoothly approaches the $\delta = 0$ solution.

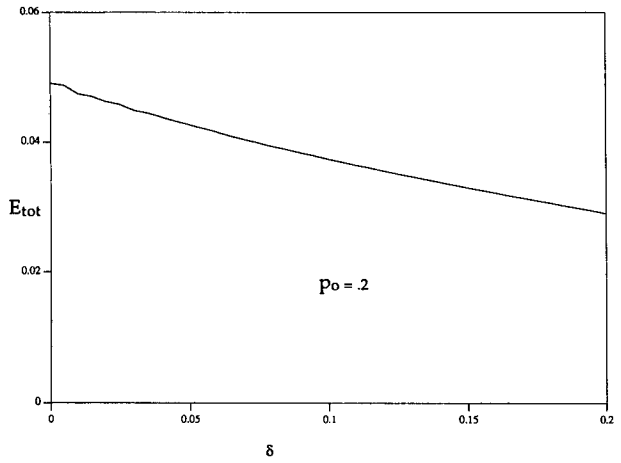

FIG. 5. Total available energy for $p_0 = 0.2$ as a function of δ. Note that energy for small δ smoothly approaches the $\delta = 0$ energy.

contains the remaining energy. We adopt the point of view here that processes present in the laboratory, such as friction, gravity waves on a free surface, or breaking interfacial waves (as indicated by preliminary numerical experiments), can efficiently remove energy from the adjusting eddy, which subsequently relaxes to the steady solutions calculated within the present highly idealized framework. Another interpretation is that our assumption that the end state of collapse is a steady axisymmetric vortex is incorrect. This point will be considered in the next section.

The above arguments are offered as evidence that the properties of a collapse eddy are not overly sensitive to the presence or absence of a cap. [The same can be shown analytically to be true in the two-dimensional case (see the Appendix).] This encourages a comparison between these solutions and the eddies formed in the laboratory by the cylinder collapse method. To this end the eddies formed by Nof and Simon (1987) (see their Fig. 5b) have some visual similarity to the small δ solutions in Fig. 4. Both extend vertically a significant fraction of the total fluid depth, and the structure of the thermocline in the capped region is significantly different from that outside the cap fluid.

3. Mixed eddy structure

Plots of $E(2p_0, \delta)$ and $2E(p_0, \delta)$ against p_0 for the choice $\delta = 0.05$ are shown in Fig. 6 [E has been calculated using (28)]. Note that two collapse eddies characterized by a given p_0 and δ have the same volume and potential vorticity character as a single collapse eddy characterized by $2p_0$ and δ. Therefore, Fig. 6 demonstrates conclusively for $\delta = 0.05$ that $E(2p_0, 0.05) > 2E(p_0, 0.05)$, or that a collapse eddy is energetically prohibited from being the end product of a free merger of two collapse eddies. (Implicit in this statement and in the analysis to follow is the assumption that all of the mass in the two collapse eddies ends up in the merged eddy.) Further, this result is not restricted to $\delta = 0.05$; rather, it has been found for all δ values examined in this study. The Nof and Simon (1987) laboratory experiments, however, clearly show merger of two eddies, which prior to merger very much resemble collapse eddies. The merged eddy must thus have some structure other than that of a collapse eddy.

Nof and Simon (1987) and Nof (1988) suggest that vortex merger is carried out by the eddies entwining each other and that the nose regions of the tentacles move in shocks. Such areas are capable of altering the potential vorticity within the cold eddy, and by sacrificing potential vorticity conservation energetically allowable eddy states can be realized.

Here, we propose a different merger pathway based on a simple parameterization of mixing. Consider two collapse eddies on the verge of an interaction (see Fig. 7a.). Since the warm water outside the eddy boundary is motionless the eddies can remain in this state indefinitely. Suppose, however, that these eddies begin to join somewhere (initiated perhaps by some external perturbation, weak friction, or instability process that causes them to overlap a small amount). The velocity structure of the warm layer of the collapse eddies is such that a discontinuity develops and this is presumably unstable. Hence, it is postulated that mutual entrainment in the warm layer over the eddies begins as the resultant instabilities grow. A detailed description of the resulting flow is virtually impossible to provide, but it seems reasonable to assume that all regions of the warm fluid over the eddies experience some effects if the cold eddies merge completely, as in Fig. 7b. Note that water with potential vorticity δ^{-1} is stirred together with water of potential vorticity 1. This interaction is also decidedly asymmetric so that angular momentum conservation by fluid parcels can no longer be invoked.

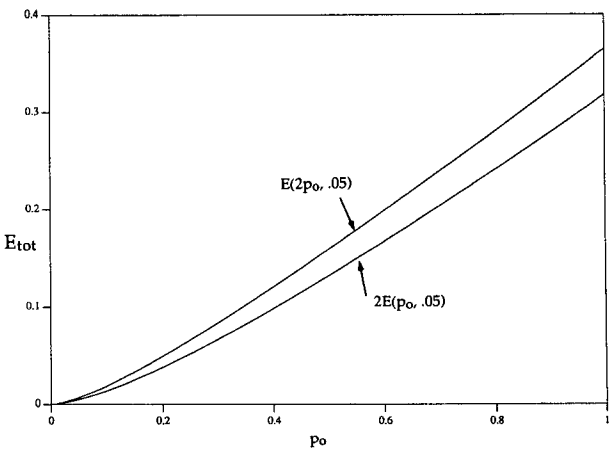

FIG. 6. The total energy in two collapse eddies of initial radius denoted by p_0 is compared to the total energy of one collapse of initial radius $2p_0$. The quantity $\delta = 0.05$. Note that the $2p_0$ eddy is energetically prohibited from being an end-state of eddy merger.

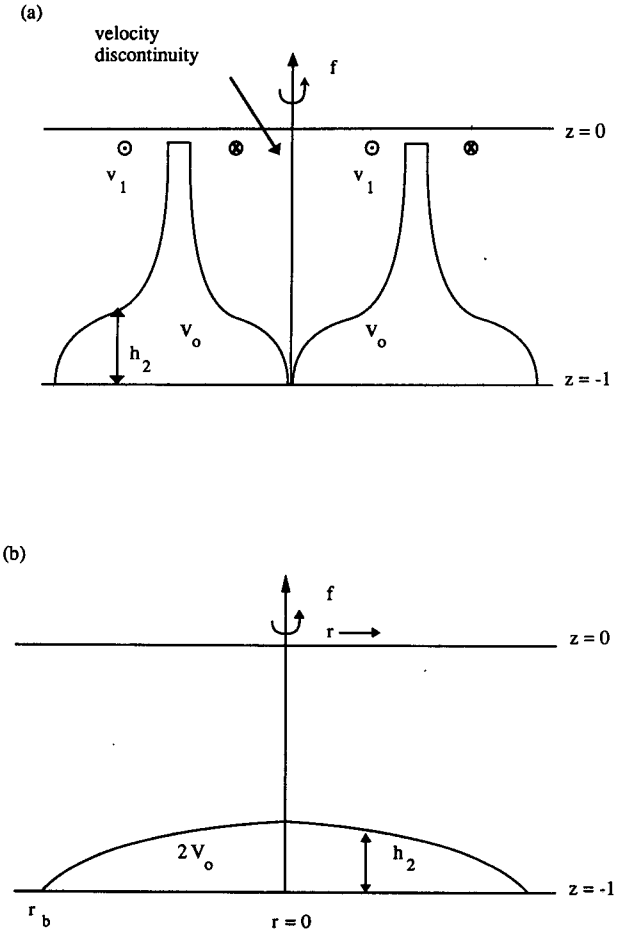

FIG. 7. Collapse eddy to mixed eddy merger schematic. The initial state is shown in (a). Note the presence of the velocity discontinuity in the warm fluid. Presumably the associated instability induces mixing. The final state can look as indicated in (b).

Assuming that the system settles again to steady state like that in Fig. 7b, the potential vorticity distribution above the eddy will have been altered from its previous discontinuous profile to some other profile. This final potential vorticity profile will depend on the details of the merging process and is impossible to specify. On the other hand, assuming the potential vorticity P is simply stirred, the volume averaged potential vorticity above the final eddy can be calculated from the initial potential vorticity distributions and is

$$\frac{2(p_0\delta)\delta^{-1} + (V - 2p_0\delta)}{V} = Q \qquad (29)$$

where V denotes the volume of warm water above the final eddy.

Since the current problem is not singular with respect to δ, the $\delta = 0$ case can be represented as the limit of vanishing δ. Thus, assuming that mixing two $\delta = 0$ collapse eddies results in a steady structure like that in Fig. 7b, (29) can still be used to calculate Q. Note that Q is greater than one, consistent with mixing high potential vorticity water (of value $P = \delta^{-1}$) with background water of potential vorticity $P = 1$. In some sense the most important role of mixing in the present scenario is that it redistributes potential vorticity, but neither creates nor destroys P. By the same reasoning the potential vorticity value within the cold eddy remains unchanged and equal to $(1 - \delta)^{-1}$.

The value of Q in (29) has the special and important property that it is consistent with vanishing swirl velocity at the eddy boundary. To see this we begin with the general warm water potential vorticity equation with an arbitrary P distribution:

$$\frac{1}{r}\frac{\partial}{\partial r} rv_1 + 1 = Ph_1. \qquad (30)$$

Upon integration (30) becomes

$$r_b v_1(r_b) + \frac{r_b^2}{2} = \bar{P}V \qquad (31)$$

where the boundary condition $v_1(0) = 0$ has been used and r_b denotes the radius of the final cold eddy. Here $\bar{P}$ denotes the volume averaged warm water potential vorticity. Substituting for $\bar{P}$ with (29) yields $v_1(r_b) = 0$.

The latter result is of critical importance. To see this, consider (30) outside the cold eddy where $P = 1$. The solution of (30) then yields

$$v_1 = C/r \qquad (32)$$

where the constant of integration, C, is fixed by requiring continuous velocity at the eddy boundary. If $v_1(r_b)$ does not vanish, the field outside the eddy will have infinite kinetic energy, and this is not acceptable.

Therefore, the process of redistributing (but not destroying) potential vorticity during vortex merger results in a P field consistent with finite energy. What remains is to calculate the energetics of such mixed eddies to see if they represent allowable end states for vortex merger.

It is likely the case that the final mixed P distribution is not unique (due to random mixing). We, therefore, arbitrarily choose to study two end states characterized by (1) $v_1 = 0$ everywhere and (2) P = constant above the eddy. The vanishing upper layer velocity case is consistent with a potential vorticity distribution of h_1^{-1} and satisfies (29). Such an eddy will obviously have finite energy. The case of constant, but unknown, potential vorticity is consistent with certain recently advanced theories of mixing in a sheared mean field, and is thus suggested as a plausible end state. We nonetheless stress that with these choices we can only argue feasibility.

The structure equation for case (1) is obtained by using the appropriate forms of (2), (3), and (27). It is simple to solve this set numerically subject to a specification of $h_1(0)$, which may then be adjusted until the cold eddy volume achieves the desired value. The

constant potential vorticity case constitutes an eigenvalue problem for P. The appropriate P value is the one that meets the conditions of vanishing v_2 at 0 and r_b and which yields the required volume of cold water in the lens. Both eddy states were calculated by straightforward shooting methods.

Examples of the thermocline structure for both mixed eddy types are shown in Fig. 8 for the case $p_0 = 0.2$ and $\delta = 0$. The collapse eddy of one-half the volume (i.e., characterized by $p_0/2$) is also shown for comparison. The comparison is made as the half-volume collapse eddy is presumably a precursor of the mixed eddies. Note the significantly different height field of the mixed eddies compared to the collapse eddy.

The total available energy for mixed eddies is given by (28) and has been computed for several values of p_0 and δ. In Fig. 9a plots of $E(p_0, \delta = 0)$ for both mixed eddy types are compared to $2E(p_0/2, 0)$, calculated using the collapse eddy solution. The energy in the two precursor collapse eddies [represented by $2E(p_0/2, 0)$] is generally greater than the energy in the one mixed eddy of either constant P or vanishing v_1 [represented by the $E(p_0, 0)$ lines], which can be formed from them in a mass conserving merger. This provides evidence that the mixed eddy states constitute energetically allowable end states of vortex merger. (For the sake of argument here, we interpret a net energy deficit to indicate an acceptable end state, appealing to viscosity or barotropic Poincare waves to remove the energy in the laboratory setting.) This result is also not confined to $\delta = 0$. Initial and final energy comparisons for $\delta = 0.05$ and $\delta = 0.1$ are provided in Figs. 9b, c.

Not all p_0, δ combinations result in energetically acceptable end states. For example, in Fig. 9b the mixed eddies appropriate to very small values of p_0 have more energy than the postulated half volume eddies (this is

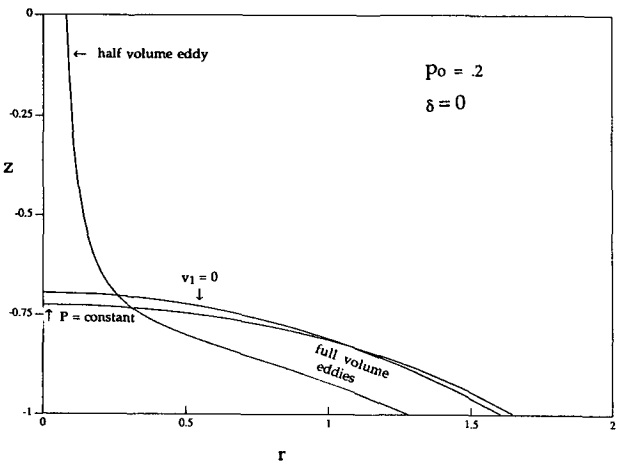

FIG. 8. Mixed eddy structures with $v_1 = 0$ and uniform potential vorticity. Also shown is the half volume collapse eddy, which is a possible precursor of the mixed eddies. The mixed eddies are characterized by $p_0 = 0.2$, $\delta = 0$.

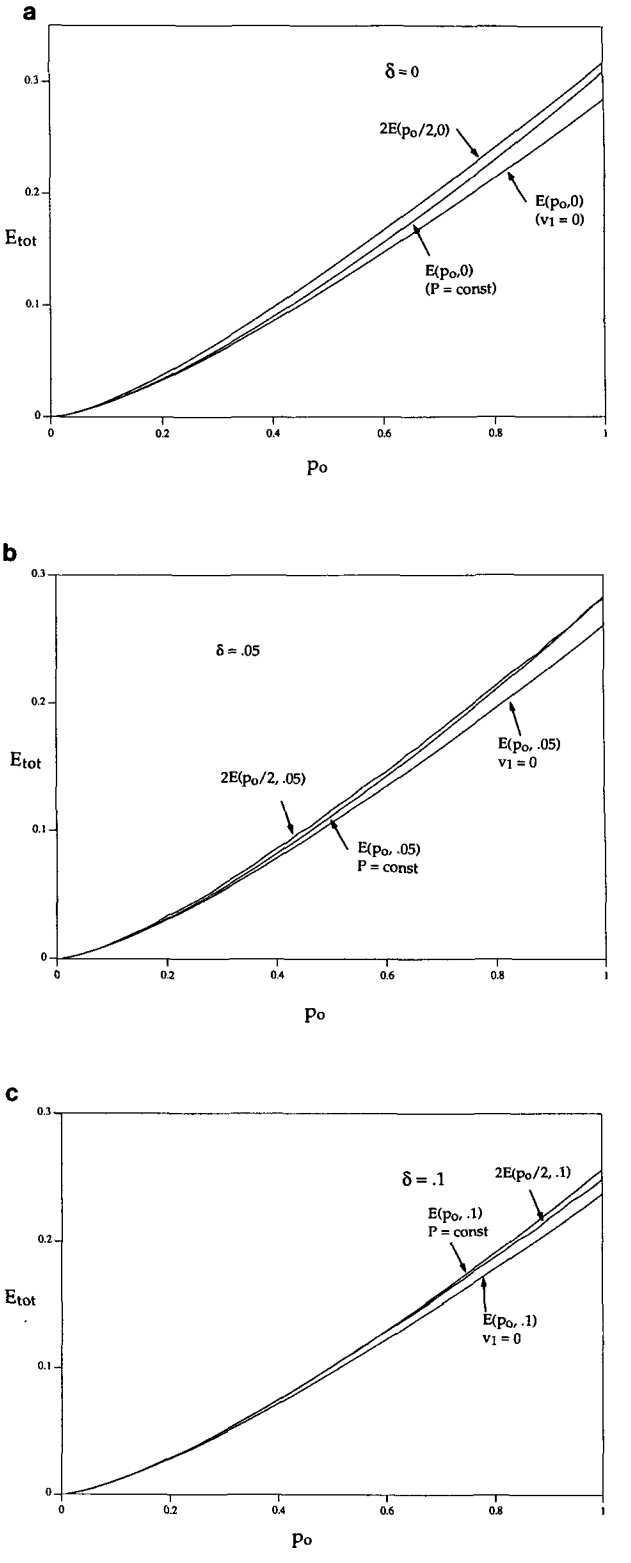

FIG. 9. Comparisons of the total available energy in two half-volume collapse eddies, characterized by $p_0/2$, versus energy in the mixed eddy characterized by p_0. The quantity $\delta = 0$ in (a), 0.05 in (b) and 0.1 in (c). Note that mixed eddies generally constitute an energetically acceptable end state for vortex merger.

not clear from the figure, but emerges clearly from the calculations). Eddies of moderate p_0 (given approximately by $p_0 > \delta$) are energetically acceptable, however. For larger p_0 ($p_0 \gtrsim 0.9$) the constant potential vorticity state is seen to be unacceptable, although the $v_1 = 0$ state remains a possibility. Comparable results apply to the case considered in Fig. 9c. It is found numerically that a midrange of p_0 results in energetically acceptable mixed eddies of both types while for $p_0 \gtrsim 0.6$ the constant potential vorticity case is excluded. Figure 9c also shows that at large p_0, the difference between the $v_1 = 0$ case and the precursor collapse eddies is decreasing. Eventually the $v_1 = 0$ state becomes unacceptable.

Figures 9b and 9c demonstrate the existence of a parameter range for which free merger is permissible. The range of acceptable p_0 is finite but characterized crudely at its low end by $p_0 > \delta$. This underscores the importance of the warm layer in the present calculations. The relation $p_0 < \delta$ corresponds to cases where the adjustment has minimal impact on the warm layer, and the collapse eddy moves toward a reduced gravity state where it is known that free merger is not energetically possible. Significant kinetic and potential energies associated with strong upper layer flows are required for the energy prohibition to be overcome.

Based on these calculations, a feasible scenario for eddy merger is as follows. Two eddies meet, each possessing significant flows in their exterior. The subsequent interaction results in potential vorticity mixing that can have the effect of altering the momentum distribution in the exterior. This can be consistent with the release of considerable kinetic energy. Disturbing the integrity of the exterior flow can also cause the release of significant potential energy through the thermal wind equation. The levels of both energies change considerably during the merger, with the resulting single eddy end state possessing less total energy than the initial two eddy state.

The effects of asymmetry

During the course of our deliberations we uncovered a separate characteristic pertaining to the energetics of eddies that might apply to the merger problem. At the risk of losing continuity with the remainder of the paper, we present here these calculations. The focus of the previous sections has been to determine if it is energetically possible for eddies with significant flows in both layers to merge into eddies with radial symmetry. In this section we revisit the question of the merger of reduced gravity eddies, and ask if the end state can be a reduced gravity eddy that lacks radial symmetry (and is, hence, presumably unsteady). In contrast with the rest of the paper, the present calculations are carried out in a reduced gravity framework and thus neglect interactions with exterior flow.

The calculations in this section will be based on the exact solutions for a reduced-gravity, elliptical vortex, presented recently by Cushman-Roisin et al. (1985). Such eddies differ from the previous eddies in that they do not have, nor can they apparently be generalized analytically to have, uniform potential vorticity. However, the Cushman-Roisin et al. solutions are at least indicative of what are possibly rather general aspects of eddy structure. We briefly outline the calculation. Interested readers are referred to the original Cushman-Roisin et al. paper for more detail. In particular, we shall use their solutions (31)–(37), and their notation in what follows.

Suppose that the total volume V and integrated potential vorticity P are given for the one-layer ellipse. We first note that changing V to some V' corresponds to rescaling P and the total energy E so that without loss of generality we can take V to be any convenient value; here we use 4π. The Cushman-Roisin et al. solution is given in terms of a single parameter δ, assuming the integrated potential vorticity is known. This determines the two amplitudes A_0 and A_1 as well as the central vortex depth. Using the formulae in their appendix for integrated volume, potential vorticity and energy, their system reduces to

$$A_0 = \delta(\delta^{1/2}P/(4\pi) - \sqrt{1+\delta} - \sqrt{1-\delta})/[\sqrt{1-\delta} - \sqrt{1+\delta}] \quad (33)$$

$$\alpha = A_1/A_0 = [1 - \delta^2/(64A_0^2)]^{1/2} \quad (34)$$

for $0 < \delta < \delta_{\max}$, where

$$\delta_{\max} = 1\Big/\left[1 + \left(\frac{P}{8\pi}\right)^2\right]. \quad (35)$$

For a given δ, the other quantities used by Cushman-Roisin et al., namely Ω and W can be computed, and the integrated energy calculated from

$$E = (64\pi/3\delta^{3/2}) \times \left[2(A_0\Omega^2 + 2\Omega A_1 W + A_0 W^2) + \frac{\delta^2}{16}\right]. \quad (36)$$

It is straightforward to show that E is a maximum for $\delta = \delta_{\max}$, which corresponds to $A_1 = 0$ and a circular vortex, and that E decreases to zero when $A_1 = A_0$ at $\delta = 0$, which corresponds to an infinitely thin and infinitely long ellipsoid.

A graph of E for varying α (which measures eddy ellipticity, circular eddies have $\alpha = 0$) is given in Fig. 10 for various values of integrated potential vorticity P. It is clear that asymmetric eddies with a given volume and P possess less energy than symmetric eddies. Thus, it is possible that part of the solution of the energy dilemma can be found by permitting the final merged eddy to be slightly asymmetric. Although no quantitative comparison can be made, it is worth noticing that the excess amount of energy present in the radially symmetric end state in Fig. 6 could be accounted for according to Fig. 10 if the end state were asymmetric.

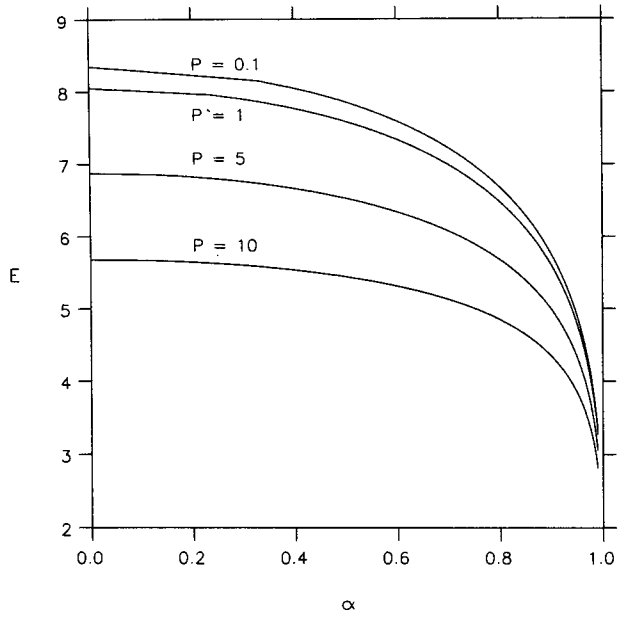

FIG. 10. Integrated energy E for the one-layer elliptical eddy of Cushman-Roisin et al. (1985), as a function of alpha, a measure of the ellipticity. Curves are given for various scaled values of P, the integrated potential vorticity of the eddy.

This is particularly true for smaller values of P (the values chosen for Fig. 10 correspond, after rescaling, to the ranges of p_0 used in Fig. 6, with increasing P corresponding to increasing p_0).

It is also possible that both mechanisms proposed in this paper (i.e., external flow mixing and the production of asymmetric, time dependent eddies) can simultaneously impact vortex merger.

4. Discussion

The previous calculations demonstrate that vortex merger in which mass and potential vorticity conservation is enforced can be energetically permissible. It has been necessary to take into account either exterior flows and their effect on thermocline structure or the effects of asymmetry. Most importantly, in the former the role of potential vorticity mixing, here parameterized as a simple volume averaging, has been emphasized. We have shown that altering the potential vorticity distribution in the exterior fluid from a discontinuous profile, like that in the collapse eddy, to a smoother profile, like those of either of the mixed eddy states, can result in a relatively low energy eddy end state. Further, we have suggested that the mixing should occur as a natural consequence of merger, due to the appearance of presumably unstable velocity discontinuities in the exterior fluid.

A natural question to ask is whether either scenario explains any laboratory vortex merger experiments. To this end we argue that certain features of the Nof and Simon (1987) experiments are reminiscent of the mixed eddy scenario. (We are unable to address the feasibility of the asymmetric scenario from the experiments documented in the literature.) The reader is referred to Figs. 5 and 6 from Nof and Simon for the purpose of this discussion.

The rough comparison of the thermocline structure of the capped collapse eddy in section 2 and the eddies soon after formation in Fig. 5b from Nof and Simon has already been pointed out. Note also the "bubble" located on top of both "collapse" eddies. Nof and Simon argue that this bubble is a result of the fluid properties of their mixture and, at least at the beginning of the experiment, marks the boundary between their "cap" and exterior warm fluid. As merger proceeded, the bubbles became disassociated from the eddies until (as in their Fig. 6) the bubbles occupied a relatively small volume of the fluid above the lens. The authors remark that the behavior of the bubbles is complicated by the mixture properties and evaporation. However, it is possible that some of the bubble evolution is indicative of the mixing of exterior and cap fluid, a feature incorporated in our model. It is also apparent that the maximum thickness of the merged eddy is significantly less than either collapse eddy in spite of the fact that the merged eddy has twice the volume. This structural feature is argued by Nof to be a reflection of the alteration of eddy potential vorticity. We point out that the mixed eddies we calculate are also much less thick than their precursor one-half volume collapse eddies. Indeed, the potential energy release associated with this structural change is one of the key facets of our scenario which makes it an acceptable one. In summary, it appears that the Nof and Simon vortex merger experiments are possibly understood within our proposed framework.

A point of contact of the calculations with the ocean is less obvious due in part to the present level of uncertainty surrounding the exterior velocity structure of field vortices. Nonetheless, what little evidence there is points to significant exterior flows near eddies (i.e., see Joyce and McDougall 1989, for a warm ring example) so we suggest that this mechanism of mixing, which releases both potential and kinetic energy, could influence the interaction of like signed oceanic vortices.

Acknowledgments. The authors gratefully acknowledge several helpful conversations with Drs. Doron Nof and William Young. One of us (W.K.D.) is sponsored by NSF Grant OCE-8711030 and ONR Contracts N00014-87-J-1209 and N00014-89-J-1577. This work was begun as a result of discussions between the authors at the 1988 Woods Hole Summer GFD School.

APPENDIX

The Collapse of a Strip

Here, we consider an equivalent problem to that of the main paper, but replace the radial symmetry con-

dition with that of no variation in one cartesian direction, taken as y. We shall show that the behavior here is qualitatively different; in particular, the cold fluid can become detached from the surface. This occurs partly because of the different geometry of the system and underscores the unique constraints imposed on circular vortices.

The cold fluid initially occupies $0 \leqslant x \leqslant x_0$ with symmetry conditions on $x = 0$. After the collapse cold fluid occupies $0 \leqslant x \leqslant x_b$; the warm fluid occupies $x \geqslant x_t$. Nondimensionally, conservation of potential vorticity gives

$$1 + v_{2x} = h_2 \tag{A1}$$

$$v_{1x} = -h_2 \tag{A2}$$

and geostrophy gives

$$v_1 = P_x \tag{A3}$$

$$v_2 = P_x + 2h_{2x} \tag{A4}$$

(the coordinate x has been nondimensionalized by $[g'H/2f^2]^{1/2}$, which accounts for the factor of 2 in (A4).). Subtracting (A3) and (A4) and using (A1) and (A2) gives

$$h_{2xx} + 1/2 = h_2 \tag{A5}$$

with boundary conditions

$$h_2 = 1, \quad x = x_t \tag{A6}$$

$$h_2 = 0, \quad x = x_b. \tag{A7}$$

Write

$$x_b = x_t + D \tag{A8}$$

for convenience so that D is the width of the collapsed cold fluid. Then h_2 is given by

$$h_2 = \frac{1}{2}\{1 + \cosh(x - x_t) - [(1 + \cosh D)/\sinh D]\sinh(x - x_t)\}. \tag{A9}$$

To find D we note that v_2 must vanish at $x = x_t$, and v_1 vanishes at x_b. Addition of (A1) and (A2) connects these quantities, and after a little algebra we have

$$2(h_{2x}(x_t) + h_{2x}(x_b)) + D = 0. \tag{A10}$$

Equation (A10) simplifies to

$$D\tanh(D/2) = 2 \tag{A11}$$

or

$$D \approx D_0 = 2.4. \tag{A12}$$

Thus, the width of the collapsed region is independent of the initial width of the cold fluid. Finally, the solution is closed by requiring conservation of mass in the cold fluid

$$x_0 = x_t + \int_{x_t}^{x_b} h_2 dx \tag{A13}$$

which yields

$$x_t = x_0 - 0.5D_0. \tag{A14}$$

For this solution to exist then,

$$x_0 > 0.5D_0 = 1.2. \tag{A15}$$

What if x_0 is less than this critical value? Clearly, unlike the radially symmetric case, x_t must vanish, and the warm fluid makes its way to $x = 0$ (causing a discontinuity in, but not an infinite value of, velocity). The modifications are straightforward. We require

$$h_2 \leqslant 1, \quad h_{2x} = -x_{0/2}, \quad \text{at} \quad x = 0 \tag{A16}$$

$$h_2 = 0, \quad \text{at} \quad x = x_b = D \tag{A17}$$

$$x_0 = \int_0^D h_2 dx. \tag{A18}$$

These give

$$h = (1/2) + \left[\left(\frac{x_0}{2}\right)\tanh D - 1/(2\cosh D)\right] \times \cosh x - \left[\frac{x_0}{2}\right]\sinh x \tag{A19}$$

$$x_0 = (D\cosh D - \sinh D)/(1 + \cosh D) \tag{A20}$$

and the first of (A16) bounds x_0:

$$x_0 \leqslant (\cosh D + 1)/\sinh D. \tag{A21}$$

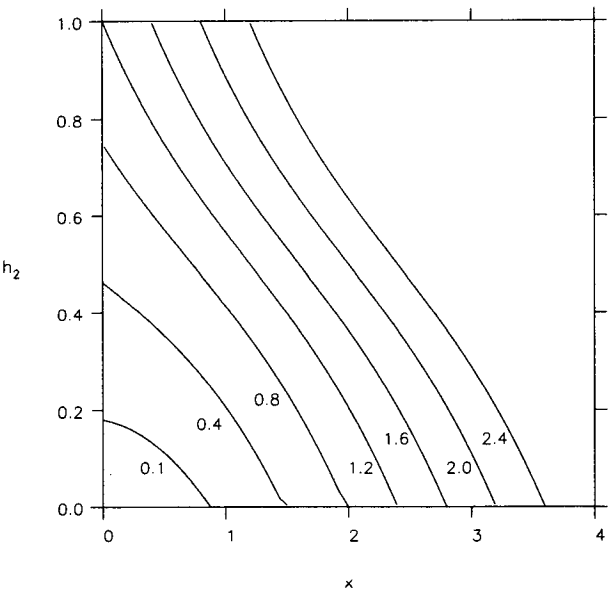

FIG. A1. The two-dimensional collapse eddy structure versus longitudinal position x. For values of x_0 less than 1.2, the lower layer subducts.

This bound gives, naturally

$$D \leqslant D_0, \quad x_0 \leqslant (1/2)D_0 \qquad \text{(A22)}$$

so that this solution is consistent and joins smoothly onto the wider one above. Figure A1 shows some profiles for varying x_0.

A treatment similar to that for the radial problem can be made for a capped eddy. It can be shown straightforwardly that as the thickness of the cap tends to zero the solution tends asymptotically to that of no cap. In particular for capped eddies, the cold fluid always separates by an O(1) amount from the surface when x_0 is less than $0.5D_0$. This is unlike the radial case, in which capped eddies with small p_0 and δ separate only a very small amount from the surface.

REFERENCES

Cresswell, G. R., 1982: The coalescence of two East Australian Current warm-core eddies. *Science,* **215,** 161–164.

Cushman-Roisin, B., 1989: On the role of filamentation in the merging of anticyclonic lenses. *J. Phys. Oceanogr.,* **19,** in press.

——, W. H. Heil and D. Nof, 1985: Oscillations and rotations of elliptical warm-core rings. *J. Geophys. Res.,* **90,** 11,756–11,764.

Gill, A., and R. Griffiths, 1981: Why should two anticyclonic eddies merge? *Ocean Modelling,* **41,** 10.

Griffiths, R., and E. Hopfinger, 1986: Experiments with baroclinic vortex pairs in a rotating fluid. *J. Fluid Mech.,* **173,** 501–518.

——, and ——, 1987: Coalescing of geostrophic vortices. *J. Fluid Mech.,* **178,** 73–97.

Joyce, T. M., 1985: Gulf Stream warm-core ring collection: An introduction. *J. Geophys. Res.,* **90,** 8801–8802.

——, and T. McDougall, 1990: Physical structure and temporal evolution of Gulf Stream warm core ring 82-B. *Deep-Sea Res.,* in press.

McWilliams, J. C., E. D. Brown, H. L. Bryden, C. C. Ebbesmeyher, B. A. Elliott, R. H. Heinmiller, B. Lien Hua, K. D. Leaman, E. J. Lindstrom, J. R. Luyten, S. E. McDowell, W. Breckner Owens, H. Perkins, J. F. Price, L. Regier, S. C. Riser, H. T. Rossby, T. B. Sanford, C. Y. Shen, B. A. Taft and J. C. Van Leer, 1983: The local dynamics of eddies in the Western North Atlantic. *Eddies in Marine Science.* A. R. Robinson, Ed., Springer-Verlag, 92–113.

Melander, M., N. Zabusky and J. McWilliams, 1988: Symmetric vortex merger in two dimensions: causes and conditions. *J. Fluid Mech.,* **195,** 303–340.

Mied, R., and G. Lindermann, 1984: Mass transfer between Gulf Stream rings. *J. Geophys. Res.,* **89,** 6365–6372.

Nof, D., 1988: The fusion of isolated nonlinear eddies. *J. Phys. Oceanogr.,* **18,** 887–905.

——, and L. Simon, 1987: Laboratory experiments on the merging on nonlinear anticyclonic eddies. *J. Phys. Oceanogr.,* **17,** 343–357.

Overman, E., and N. Zabusky, 1982: Evolution and merger of isolated vortex structures. *Phys. Fluids,* **23,** 2339–2342.

Smeed, D. A., 1987: A laboratory model of benthic fronts, *Deep-Sea Res.,* **34**(8), 1431–1460.